Carbon Dioxide Capture for Storage in Deep Geologic Formations – Results from the CO_2 Capture Project

Geologic Storage of Carbon Dioxide with Monitoring and Verification

Volume 2

Elsevier Internet Homepage – http://www.elsevier.com
Consult the Elsevier homepage for full catalogue information on all books, major reference works, journals, electronic products and services.

Elsevier Titles of Related Interest

AN END TO GLOBAL WARMING
L.O. Williams
ISBN: 0-08-044045-2, 2002

FUNDAMENTALS AND TECHNOLOGY OF COMBUSTION
F. El-Mahallawy, S. El-Din Habik
ISBN: 0-08-044106-8, 2002

GREENHOUSE GAS CONTROL TECHNOLOGIES: 6TH INTERNATIONAL CONFERENCE
John Gale, Yoichi Kaya
ISBN: 0-08-044276-5, 2003

MITIGATING CLIMATE CHANGE: FLEXIBILITY MECHANISMS
T. Jackson
ISBN: 0-08-044092-4, 2001

Related Journals:
Elsevier publishes a wide-ranging portfolio of high quality research journals, encompassing the energy policy, environmental, and renewable energy fields. A sample journal issue is available online by visiting the Elsevier web site (details at the top of this page). Leading titles include:

Energy Policy
Renewable Energy
Energy Conversion and Management
Biomass & Bioenergy
Environmental Science & Policy
Global and Planetary Change
Atmospheric Environment
Chemosphere – Global Change Science
Fuel, Combustion & Flame
Fuel Processing Technology

All journals are available online via ScienceDirect: www.sciencedirect.com

To Contact the Publisher
Elsevier welcomes enquiries concerning publishing proposals: books, journal special issues, conference proceedings, etc. All formats and media can be considered. Should you have a publishing proposal you wish to discuss, please contact, without obligation, the publisher responsible for Elsevier's Energy program:

Henri van Dorssen
Publisher
Elsevier Ltd
The Boulevard, Langford Lane
Kidlington, Oxford
OX5 1GB, UK

Phone: +44 1865 84 3682
Fax: +44 1865 84 3931
E.mail: h.dorssen@elsevier.com

General enquiries, including placing orders, should be directed to Elsevier's Regional Sales Offices – please access the Elsevier homepage for full contact details (homepage details at the top of this page).

Carbon Dioxide Capture for Storage in Deep Geologic Formations – Results from the CO_2 Capture Project

Geologic Storage of Carbon Dioxide with Monitoring and Verification

Edited by

Sally M. Benson
Lawrence Berkeley Laboratory
Berkeley, CA,USA

and Associate Editors

Curt Oldenburg[1], Mike Hoversten[1] and Scott Imbus[2]
[1]Lawrence Berkeley National Laboratory
Berkeley, CA, USA
[2]Chevron Texaco Energy Technology Company
Bellaive, TX, USA

Volume 2

ELSEVIER
2005

Amsterdam – Boston – Heidelberg – London – New York – Oxford
Paris – San Diego – San Francisco – Singapore – Sydney – Tokyo

ELSEVIER B.V.
Radarweg 29
P.O. Box 211, 1000 AE Amsterdam
The Netherlands

ELSEVIER Inc.
525 B Street, Suite 1900
San Diego, CA 92101-4495
USA

ELSEVIER Ltd
The Boulevard, Langford Lane
Kidlington, Oxford OX5 1GB
UK

ELSEVIER Ltd
84 Theobalds Road
London WC1X 8RR
UK

First edition 2005

Library of Congress Cataloging in Publication Data
A catalog record is available from the Library of Congress.

British Library Cataloguing in Publication Data
A catalogue record is available from the British Library.

ISBN: 0-08-044570-5 (2 volume set)

Volume 1: Chapters 8, 9, 13, 14, 16, 17, 18, 24 and 32 were written with support of the U.S. Department of Energy under Contract No. DE-FC26-01NT41145. The Government reserves for itself and others acting on its behalf a royalty-free, non-exclusive, irrevocable, worldwide license for Governmental purposes to publish, distribute, translate, duplicate, exhibit and perform these copyrighted papers. EU co-funded work appears in chapters 19, 20, 21, 22, 23, 33, 34, 35, 36 and 37. Norwegian Research Council (Klimatek) co-funded work appears in chapters 1, 5, 7, 10, 12, 15 and 32.

Volume 2: The Storage Preface, Storage Integrity Preface, Monitoring and Verification Preface, Risk Assessment Preface and Chapters 1, 4, 6, 8, 13, 17, 18, 19, 20, 21, 22, 23, 24, 25, 26, 27, 28, 29, 30, 31, 32, 33 were written with support of the U.S. Department of Energy under Contract No. DE-FC26-01NT41145. The Government reserves for itself and others acting on its behalf a royalty-free, non-exclusive, irrevocable, worldwide license for Governmental purposes to publish, distribute, translate, duplicate, exhibit and perform these copyrighted papers. Norwegian Research Council (Klimatek) co-funded work appears in chapters 9, 15 and 16.

♾ The paper used in this publication meets the requirements of ANSI/NISO Z39.48-1992 (Permanence of Paper).
Printed in The Netherlands.

Carbon Dioxide Capture for Storage in Deep Geologic Formations, Volume 2
D.C. Thomas and S.M. Benson (Eds.)

Chapter 32

CO_2 STORAGE IN COALBEDS: RISK ASSESSMENT OF CO_2 AND METHANE LEAKAGE

Shaochang Wo[1], Jenn-Tai Liang[2] and Larry R. Myer[3]

[1]Institute for Enhanced Oil Recovery and Energy Research, University of Wyoming,
1000 E University Ave, Dept 4068, Laramie, Wyoming, 82071
[2]The University of Kansas, Lawrence, KS 66045, USA
[3]Lawrence Berkeley National Laboratory, Berkeley, CA 94720, USA

ABSTRACT

The practice of testing seal integrity is not routinely employed in coalbed methane projects. With injection of CO_2, changes in stress caused by potential high injection pressure and rate may open previously closed fractures and faults, thus generating new leakage pathways. The research presented in this chapter focuses on assessing potential leakage pathways and developing a probabilistic risk assessment methodology. A study was performed to evaluate geomechanical factors that need to be taken into account in assessing the risk of CO_2 leakage in CO_2 storage in coalbeds. The study revealed that geomechanical processes lead to risks of developing leakage paths for CO_2 at each step in the process of CO_2 storage in coalbeds. Risk of leakage is higher for old wells that are converted to injectors. Risks of leakage are much higher for open cavity completions than for cased well completions. The processes of depressurization during dewatering and methane production, followed by repressurization during CO_2 injection, lead to risks of leakage path formation by failure of the coal and slip on discontinuities in the coal and overburden. The most likely mechanism for leakage path formation is slip on pre-existing discontinuities that cut across the coal seam. A mathematical model for probabilistic risk assessment was developed. The model consists of six functional constituents: initiators, processes, failure modes, consequences (effects), indicators, and inference queries. Potential leakage pathways are usually coupled with identified failure modes. In assessing the risk of CO_2 storage in geological formations, inference rules can generally be categorized into seven different types. The inference logic of this model is based on set theory, which is superior to the traditional decision-tree based inference logic in terms of flexibility, generality, capability in dealing with uncertainties and handling large, complex problems, such as cascading phenomena. The model was designed to be implemented on a relational database.

INTRODUCTION

A recent report by Reeves [1] estimates that the total CO_2 storage potential in unmineable coalbeds in the US alone is about 90 gigatons, with the additional benefit of 152 trillion cubic feet of methane recovery. Methane production from coalbeds can be enhanced by injection of CO_2 to displace or N_2 to strip the methane from the coal and accelerate methane production at higher pressures (see Chapter 15). The mechanism by which CO_2 or N_2 can enhance the coalbed methane recovery process, and CO_2 is stored, is a complex mix of physical and chemical interactions that strive to achieve equilibrium simultaneously

Abbreviations: BP, British Petroleum; BLM, Bureau of Land Management; CCP, CO_2 Capture Project; CBM, Coalbed Methane; CRADA, Cooperative Research and Development Agreement; DOE, Department of Energy; ECBM, Enhanced Coalbed Methane Recovery; INEEL, Idaho National Engineering and Environmental Laboratory; JIP, Joint Industry Program; LBNL, Lawrence Berkeley National Laboratory; NETL, National Energy Technologies Laboratory.

in the sorbed state and the gaseous state. Coal has the capacity to hold considerably more CO_2 than either methane or nitrogen in the adsorbed state, in an approximate ratio of 4:2:1 for typical Fruitland coal in the San Juan basin [2–4]. This is because stronger forces of attraction exist between coal and CO_2 than between coal and methane or nitrogen. Two commercial demonstration projects of enhanced coalbed methane recovery (ECBM) by gas injection have been implemented at the Allison and Tiffany Units [2–6] in the San Juan basin.

Historically, methane seepage has been observed from the Pine River [7–9], South Texas Creek, Valencia Canyon, Soda Springs, and other areas [10–12] along the north and west Fruitland outcrops. Both of the Tiffany and Allison Units are located more than 15 miles away from any outcrop sites. It is very unlikely that injected CO_2 or N_2 could migrate to outcrops. However, simulation predicted that a large volume of methane and N_2/CO_2 breakthrough could occur if the N_2/CO_2 injection wells are placed too close to outcrops [13] (Chapter 15, this volume). Prior to any CO_2/N_2 being injected, methane leakage was observed in the CBM producing area. On July 23 1991, the Bureau of Land Management (BLM) issued a notice NTLMDO-91-1 in response to evidence of methane contamination in groundwater [10]. Since 1991, the BLM has aggressively implemented the terms and conditions of NTL MDO-91-1. The Colorado Oil and Gas Conservation Commission (COGCC) has also implemented and enforced similar requirements for gas wells on state and free lands. With the injection of CO_2 or N_2, the concern is that it could follow the methane leakage pathways to leak toward outcrops or the surface. In addition, repressuring coalbeds by CO_2 or N_2 injection will generate stresses and displacements in the coal seam and the adjacent overburden. The question is whether these stresses and displacements will generate new leakage pathways by failure of the rock or slip on pre-existing discontinuities such as fractures and faults.

In this study we evaluated the geomechanical factors which should be taken into account for assessing the risk of CO_2 leakage from coalbed storage projects. While conceptual and descriptive risk characterization is necessary and helpful in providing the baseline for quantitative risk assessments, decision makers need meaningful quantitative indicators, such as CO_2 leakage paths, leakage rate and volumes, CO_2 concentration at a leakage site, and remediation cost. In reality, quantifying site-specific risks is not easy. One must address uncertainties in almost all aspects of the project including site characterization, operations, and particularly in assessing the future evolution of the storage site. Probability-based risk assessment is considered as a meaningful and effective method for dealing with uncertainties. In this study, a mathematical model for probabilistic risk assessment was developed. Potential leakage pathways are assessed as failure modes. The model was designed to be implemented on a relational database.

NATURAL AND INJECTION-INDUCED LEAKAGE PATHWAYS

Coalbed reservoirs are self-contained petroleum systems, wherein the two critical petroleum system elements of source rock and reservoir rock are located together in a single geologic unit. Unlike conventional reservoirs, where gas or oil accumulated in a sedimentary porous rock below a low-permeability formation that acts as a seal, the majority of coalbed methane is adsorbed on the surface of the coal matrix and is not free to migrate until pressure is relieved by the withdrawal of water. For that reason, the seal integrity of coalbeds is generally not tested by the techniques that are used in conventional oil and gas reservoirs. In addition to naturally occurring microfractures (cleats), joints and faults may also be present in coalbeds, such as in the San Juan basin [14]. Joints and faults are larger scale fractures that typically cut across coalbeds and non-coal interbeds.

During the primary production in the San Juan Basin, methane seepage has increased at historic seepage sites. Inadequately cemented conventional gas wellbores and vertical microseepage are suspected of contributing to methane migration into surface soils and groundwater [10]. With the injection of CO_2 or N_2, the change in stress caused by high injection pressure and rate may open previously closed fractures and faults. To evaluate the geomechanical issues in CO_2 storage in coalbeds, it is necessary to review each step in the process of development of a CO_2 storage project and evaluate its geomechanical impact. A coalbed methane production/CO_2 storage project will be developed in four steps:

- drilling and completion of wells;
- formation dewatering and methane production;

- CO_2 injection with accompanying methane production; and
- possible CO_2 injection for storage only.

The approach taken in this study was to review each step, identify the geomechanical processes associated with it, and assess the risks that leakage would result from these processes.

Drilling and Completion Risks

Drilling issues

Wellbore instability is a geomechanical problem that can be encountered during drilling. Weak shale layers, weak coal layers, overpressure, and fault zones are common causes. Rock failure and displacements associated with wellbore instability generate potential leakage paths in the vicinity of the well. The risk of leakage will be minimized by cementing the casing. It is conventional practice to place cement behind production casing. Title 19 chapter 15 of the New Mexico Administrative Code states "cement shall be placed throughout all oil-and gas-bearing zones and shall extend upward a minimum of 500 ft above the uppermost perforation or, in the case of open-hole completion 500 ft above the production casing shoe". Alabama's regulations specific to coalbed methane operations have been used by other states as a model. Section 400-3 of the Rules and Regulations of the State Oil and Gas Board of Alabama states that the casing shall be cemented for 200 ft above the top of the uppermost coalbed which is to be completed, or for 200 ft above the production casing shoe in open hole completions. The production interval in cased hole completions need not be cemented.

When a coalbed methane project is converted to CO_2 storage, CO_2 will be injected under pressure. Wells used for injection in oil and gas formations are subject to additional regulations requiring periodic testing for leakage in the cased section. The type of testing which is required is set by individual states. In New Mexico, these tests can include the use of tracers to test for leakage in the annulus.

Injection of CO_2 also increases the risk of leakage in the annulus between casing and formation due to chemical dissolution of the cement. Experience in enhanced oil recovery has led to development of additives for cement used for CO_2 injectors. This experience should be applicable to coalbed methane CO_2 projects.

If old production wells or idle wells are used for CO_2 injection there is a risk that leakage paths may be present in the annular space between the casing and the rock due to deteriorated or missing cement. Casing bond logs and tracer tests can be used to evaluate the integrity of the cement in the annulus or the contact between casing and formation. If the integrity of the cement bond is inadequate, cement can be injected (squeezed) into the annulus. However, the process of seal formation in the annulus by cement squeeze behind casing is expensive and often only partially successful.

Because of the importance of the casing cement in minimizing the risk of CO_2 leakage, additional work should be directed toward development of recommendations for best practices. In particular, criteria for setting the height of the cement behind casing needs further study. Because of the substantial industry experience in water flooding and CO_2 enhanced oil recovery, a case history study of the performance of production casing cement would provide valuable data for a best practices study.

Conventional completions

A conventional completion for a coalbed methane project involves perforating or slotting the casing in the coal seam (Figure 1). Since the permeability of coal matrix is low, hydrofracturing is used to enhance permeability during dewatering and primary production. If the project is converted to CO_2 enhanced recovery and storage, pre-existing hydrofractures will enhance the injectivity of the CO_2. However, the risk of CO_2 leakage is also increased if hydrofractures extend into the overburden. Growth into the overburden can happen when the hydrofracture is initially created. In addition, since CO_2 is injected under pressure, fracture growth into the overburden could also occur during the enhanced recovery and storage phases of the project.

The potential for vertical extension of a hydraulic fracture is dependent upon several factors [15].

- *In situ stress state*. Higher horizontal stress in surrounding layers will impede vertical fracture growth, while lower horizontal stress tends to accelerate it. Higher pore pressure will enhance fracture growth.

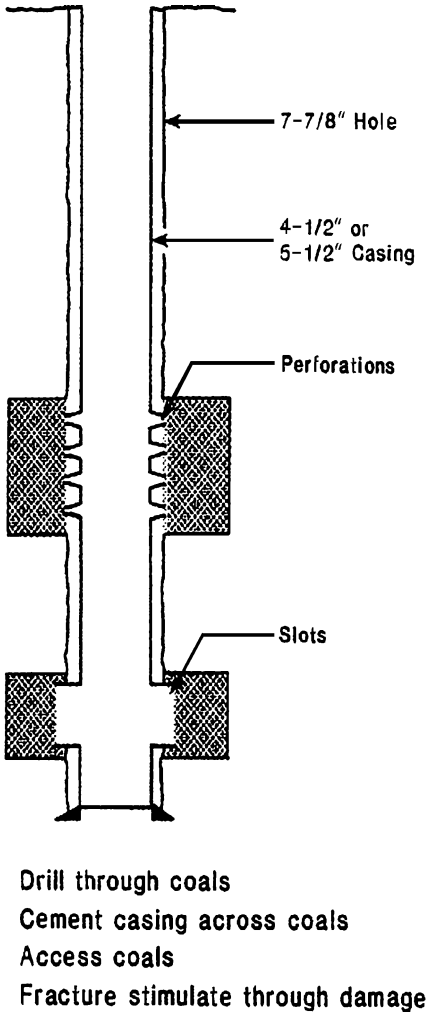

Figure 1: Schematic diagram of cased-hole completion for coalbed methane well [17].

On average, horizontal stress increases with depth but the lithology can affect in situ stress values. Pore pressures can also depart significantly from a "normal" hydrostatic gradient depending on the regional hydrologic setting as well as previous production and injection activities in the field.

- *Elastic moduli*. Vertical growth is impeded if the adjacent layer is stiffer than the coal seam. This is most likely to be the case if limestone or sandstone is the bounding strata. Siltstones and shale can vary widely in properties, but many are also stiffer than coals.
- *Toughness*. Higher fracture toughness will impede fracture growth. For large fractures, tensile strength is not a major factor [15]. The fracture toughness of coal is not well known. Atkinson and Meredith [16] compiled results of tests on four different coals. For Latrobe Valley Brown and Pittsburgh coal, values of "stress intensity resistance" ranged from 0.006 to 0.063 MPa $m^{1/2}$. However, for Queensland semi-anthracite and New South Wales black coal, values ranged from 0.13 to 0.44 MPa $m^{1/2}$. For comparison, values for sandstone, shale and limestone ranged from about 0.4 to 1.7 MPa $m^{1/2}$, with values for limestone generally being higher. This data indicates that some coals will have significantly lower

fracture toughness than typical bounding formations, and, therefore, there is a low risk of fracture growth out of interval.

- *Leakoff*. High fluid loss into the formation will retard growth of a fracture propagating into it.
- *Fluid flow*. Vertical fracture propagation will also be affected by the vertical component of fluid flow, which is affected by fracture opening and fluid properties. The effects of the fluid properties of CO_2 (particularly the non-wetting characteristics) on fracture propagation are a topic for further research.

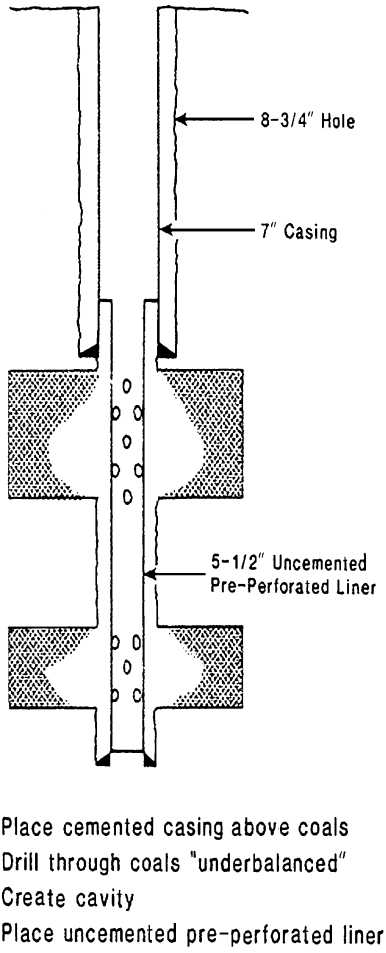

Figure 2: Schematic diagram of cavity completion for coalbed methane well [17].

Linear elastic fracture mechanics models have been developed to predict vertical fracture growth [18]. Ahmed et al. [19] developed expressions specifically for design in multiple zones. The approach is to first calculate the stress intensity factors for the top and bottom of the fracture. The stress intensity factor is a function of the height of the fracture the in situ horizontal effective stress, and the fluid pressure in the fracture. Fracture growth is predicted when the stress intensity factor exceeds a critical value given by the fracture toughness of the rock.

Risk of leakage will be reduced if the vertical extent of hydrofractures can be monitored. In cased wells measurement of fracture height, or detection of vertical propagation into bounding formations, is a challenging undertaking. Ahmed [18] and Anderson et al. [20] describe the use of radioactive tracers in conjunction with gamma ray logging. However, this technique only provides information in the near wellbore region.

In principle, seismic methods could be used to monitor the extension of a hydrofracture. Passive seismic techniques use seismic "events" generated by the fracturing process to locate the fracture. The fracture can also be imaged by a number of active seismic techniques. Though field experiments have been conducted, there is as yet no generally accepted seismic technique for determining fracture height. Nolte and Economides [21] describe a method for interpreting the downhole pressure decline during pumping to determine if a fracture has propagated into a bounding layer. The fracture extension may, however, not be vertical. Augmenting the pressure data analysis with other techniques such as passive or active seismic imaging may provide more information on the geometry of the propagating fracture.

Open cavity completions

A second type of completion for coalbed methane projects is the open hole cavity method (Figure 2). This technique was developed in the San Juan basin and is advantageous in areas where reservoir pressures are higher than normal. In such areas, casing is set above the coal seam and a cavity is generated by one of the two methods [22]. The first method is to drill through the coal seam underbalanced with water, air or foam. The excess formation pressure causes the coal to collapse into the wellbore. The coal is removed by displacing with drilling fluid and a perforated screen is set.

The second method uses pressure surges to collapse the coal. The well is shut in to build up pressure and then is abruptly released. Collapsed coal is then removed. This process can be repeated several times until the coal no longer collapses. Bland [22] reported that the effect could extend as much as 100 m into the coal seam.

Creation of a cavity can potentially cause failure and displacements in the overlying strata which provide pathways for CO_2, and increase the risk of leakage. Factors which influence the amount of disturbance in the overburden include the size and shape of the cavity, surge pressures, depth and in situ stress, layer thickness, rock strength and degree of natural fracturing in the overburden.

The process of pressure surging sets up high pore pressure gradients in the rock and corresponding flow lines as schematically illustrated in Figure 3a. Underbalanced drilling has the same effect though the pore pressure gradients would be lower. These pressure gradients cause fractures, joints, and cleats oriented perpendicular to the flow lines to open, leading to sloughing of the coal into the opening. The pressure gradients are also present in the overburden, so there is risk that this rock will also collapse into the cavity. The risk is highest for weak, thinly bedded, highly fractured shale. The risk is least for massively bedded sandstone and limestone.

The risk of overburden collapsing into the cavity increases as the cavity grows in width. As shown in Figure 3b of Chapter 33, removal of coal results in an unsupported span of layered overburden. As the span increases, so does the likelihood of finding fractures which define blocks. These blocks can be moved or removed by repeated surging. Since the interfaces between rock layers are weak, repeated surging would also tend to cause separation between layers producing more fluid pathways.

Creation of a cavity also results in a redistribution of the in situ stresses. This redistribution is very dependent upon the shape of the cavity as well as the relative magnitude of the vertical and horizontal far field stresses. The shape of the cavity formed by surging can be approximated by an ellipsoid with major axis equal to the thickness of the seam. The stress distribution around an elliptical (2D) cavity with major axis oriented parallel to the vertical far field stress is shown in Figure 4. It is seen that near the opening, in a direction along the minor axis the horizontal stress is less than the far field stress. Thus, the stress redistribution would be acting to further open fractures already opened by pressure surging. Similarly, along the major axis the vertical stress is less than the far field, increasing the risk that pressure surges would cause bedding plane partings.

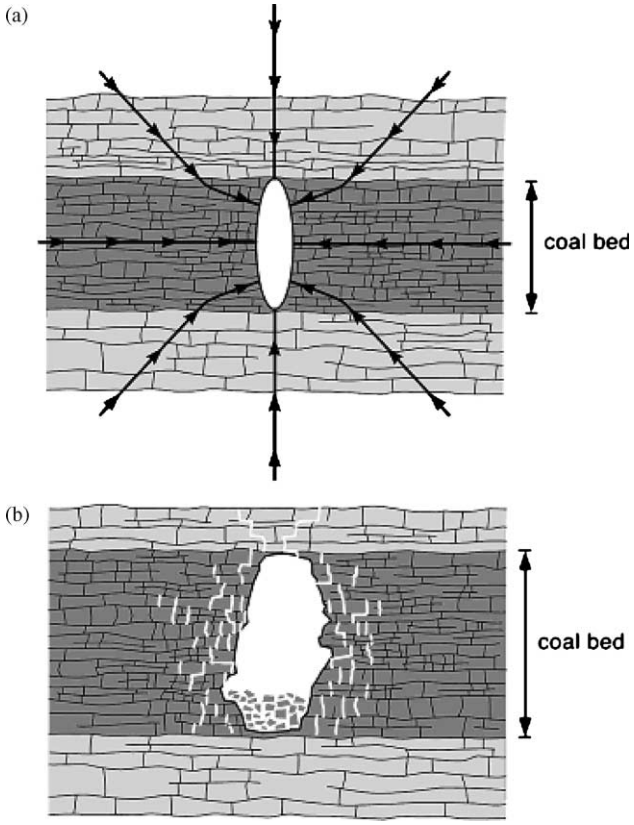

Figure 3: Schematic illustration of rock mass behavior associated with cavity completions in coalbeds. (a) Flow lines for water movement during surging. (b) Growth of cavity and fracturing in the coal and overburden.

Production and Repressurization Risks

The pore pressure reductions that occur during dewatering and methane production and pore pressure increase that occur during CO_2 injection, cause displacements in the reservoir and surrounding rock. A conservative assumption (to be discussed further) is that leakage will result if the rock fails or if slip occurs on pre-existing faults or discontinuities.

Failure and slip in a coal seam

A convenient way of assessing the potential for failure or slip is the Mohr diagram (Figure 5). A simple two-dimensional linear Mohr–Coulomb failure criterion is shown for illustration. The effective principal stress defined as total stress minus pore pressure is plotted on the horizontal axis and referred to as "normal stress". It is commonly assumed that an increase in pore pressure in the reservoir has an equal effect on both the components of principal stress, causing the Mohr circle to shift to the left, closer to failure, i.e. from I → II in Figure 5. This assumption has been employed in previous assessments of the potential for fault slip due to reservoir pressurization by CO_2 injection [25]. If pore pressures are reduced, it follows from this model that both the components of effective stress would be increased by the same amount, moving the Mohr circle away from failure.

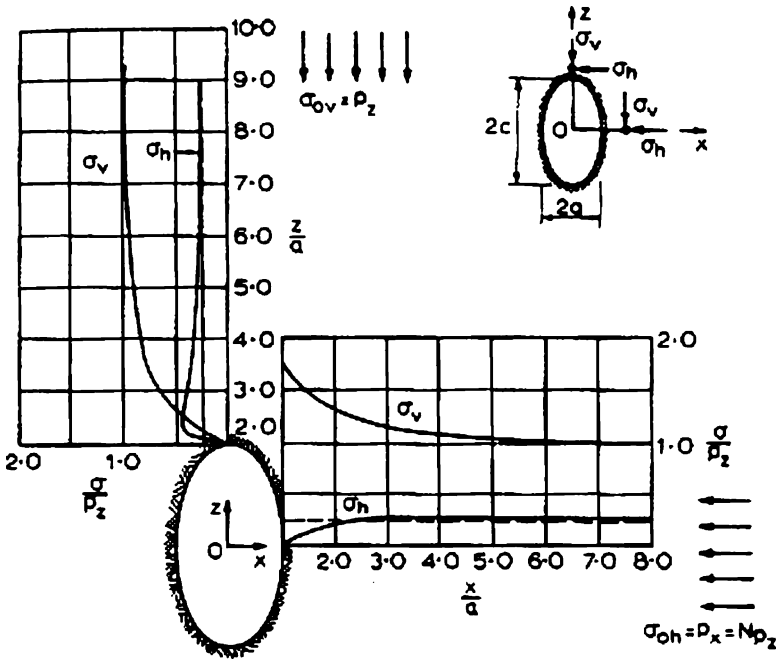

Figure 4: Stresses around an elliptical cavity $(a/c = 1/2)$ in homogeneous stress fields $(N = 0.25)$ [23,24].

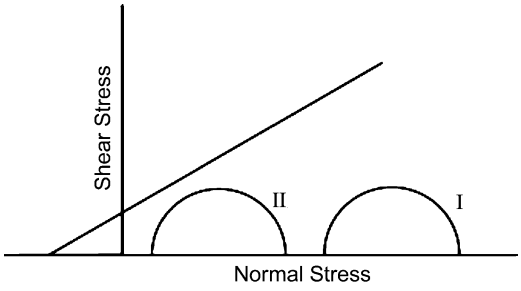

Figure 5: Mohr circles for initial (I) and final (II) stress state when it is assumed that a pore pressure increase affects both principal stresses equally.

Observations in a number of petroleum reservoirs [26,27] have shown that the reduction in pore pressure due to production causes a smaller change in horizontal stress than in vertical stress. The effect on the potential for failure is shown in Figure 6. Since pore pressures are decreasing, the Mohr circle moves to the right. However, since the change in horizontal effective stress is less than in the vertical effective stress, the circle actually gets closer to failure that is from I → III in Figure 6 of Chapter 33. Teufel et al. [28] showed that these effects were large enough to cause failure of the high porosity chalk in the North Sea Ekofisk reservoir. Streit and Hillis [29] further analyzed the effects on fault slip.

These relative changes in horizontal and vertical effective stresses are the result of the effects of far field (in situ) boundary conditions and poroelastic properties of the rock. Figure 7 shows that the rate of change

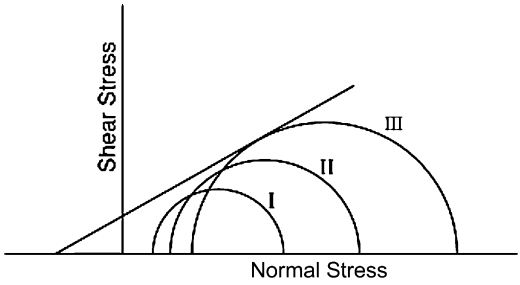

Figure 6: Mohr circles for initial (I), intermediate (II), and final (III) stress states for pore pressure reduction assuming that horizontal stresses are less affected than vertical stresses. Failure or slip occurs at III.

in horizontal stress with pore pressure, i.e. $\Delta\sigma_h/\Delta P$ where σ_h is horizontal stress and P is pore pressure, decreases as Poisson's ratio of the reservoir rock increases. Touloukian et al. [30] reported measured values of Poisson's ratio for coal of 0.2–0.4.

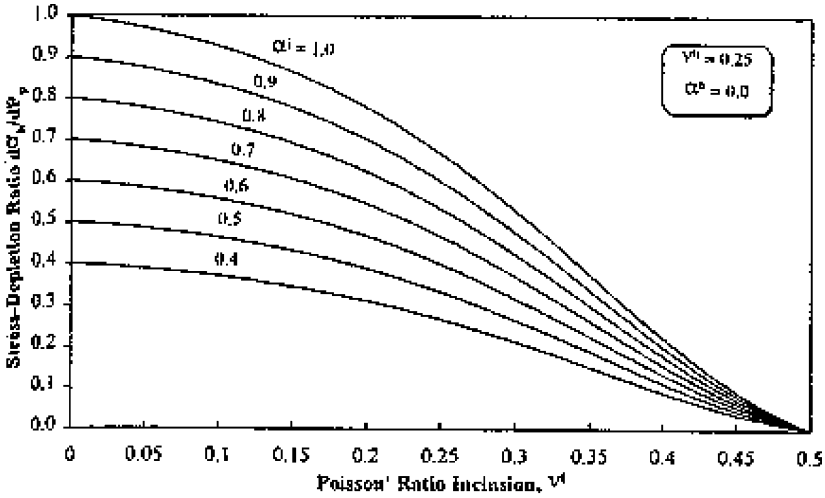

Figure 7: Effect of Poisson's ratio of the reservoir rock on rate of change in horizontal stress with pore pressure for a disc-shaped reservoir modeled as an inclusion (i) in a host (h) rock and various Biot coefficients [31].

The risk of failure or slip in the coal will depend on depth, in situ stress state, pressure drawdown, and coal strength and poroelastic properties. Conditions which result in large principal stress differences increase the risk of failure and slip. Tectonic activity will result in increased differential far field stresses. Large pore pressure drawdown will increase differential stress. Risk of failure increases for low strength coal. In situ stresses increase with depth, but the strength of rock increases with level of confinement. The risk of failure may or may not increase with depth depending on the amount of pore pressure drawdown and the magnitude of differences between components of in situ stress. The risk of slip on pre-existing discontinuities is increased for low cohesion and low frictional sliding resistance.

Injection of CO_2 for enhanced methane production and storage will increase pore pressures in the coal seam. In a poroelastic system, effective stress changes due to pore pressure drawdown are simply reversed by pore pressure increase due to injection. Thus, a Mohr circle which had moved closer to failure under drawdown would move farther from failure during injection until the original, pre-development pore pressures are obtained. Failure, however, is an inelastic process and, in general, results in a complex redistribution of stress in the system.

If pore pressures from CO_2 injection exceed pre-development levels, then there is a risk that slip will occur even though it had not occurred under drawdown conditions. This is conceptually illustrated in Figure 8, where the Mohr circle for pre-development stress state is labeled I. Dewatering and methane production moves the Mohr circle to the right (state II) under conditions in which the change in horizontal effective stress is less than the change in vertical effective stress. The maximum stress difference is not sufficient to cause failure or slip. Upon repressurization, assuming no inelastic effects, the Mohr circle returns to state I. If pressurization continues so that pore pressures rise above pre-development levels the Mohr circle moves to the left, resulting in the condition for failure or slip as indicated by state III in the figure. It has been assumed in this construction that the vertical effective stress changes more rapidly than the horizontal effective stress during pore pressure increase.

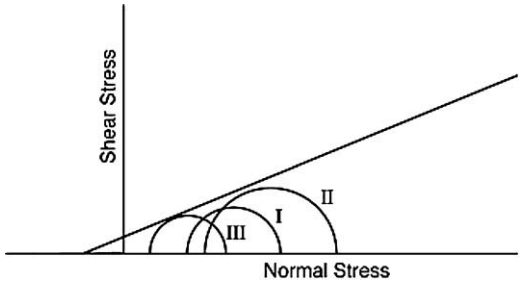

Figure 8: Mohr circles for initial (I), intermediate (II) and final (III) stress state when pore pressure first decreases (II) and then increases (III) with respect to initial conditions. Failure or slip occurs at III.

The approach outlined above can be used to make a preliminary assessment of the potential for slip on pre-existing discontinuities in the coal in the San Juan basin. Values of parameters used in the analysis are summarized in Table 1. A mean depth of 3200 ft and an initial reservoir pressure of 1500 psi before dewatering and methane production are assumed. The reservoir pressure is consistent with a normal hydrostatic gradient and observations in some areas of the San Juan basin. It is assumed that the maximum principal stress is vertical (S_V) and the density gradient is 1 psi per foot of depth. For purpose of this calculation the in situ stress, S_{hmin}/S_V, where S_{hmin} is the minimum horizontal stress, is assumed to be 0.7. The condition for slip on the discontinuity is given by a linear Mohr–Coulomb criteria with the conservative assumption that the cohesion is zero. A coefficient of friction, μ, of 0.6 is assumed. This value is frequently assumed in analyses of slip on faults in petroleum reservoirs [25,32]. It is also consistent with laboratory measurements of the strength of coal under confining pressures of several thousand psi [33].

The Mohr circle labeled by I in Figure 9 represents the initial stress conditions. It is assumed that pore pressures have equilibrated over a large area over time, so the initial major and minor principal effective stresses, σ_1 and σ_3, are given by subtracting 1500 psi from both S_V and S_{hmin}. It is then assumed that reservoir pressures are drawn down to 500 psi and there is a poroelastic effect in a finite-sized reservoir. From Figure 7, if the Poisson's ratio of the coal is 0.3, then $\Delta S_{hmin} = -0.53\Delta P$ (where P is reservoir pressure and " − " refers to a decrease in P) and the Mohr circle moves to position labeled II. As seen in the figure, there is no slip. For a Poisson's ratio of 0.4, $\Delta S_{hmin} = -0.23\Delta P$ and the Mohr circle is given by II′ which is a more stable condition than that attained for Poisson's ratio of 0.3.

TABLE 1
SLIP ANALYSIS PARAMETER

Parameter	Value
Mean reservoir depth	3200 ft
Initial reservoir pressure	1500 psi
Post drawdown reservoir pressure	500 psi
Reservoir pressure after CO_2 injection	2000 psi
Poisson's ratio for coal	0.3, 0.4
Coefficient of friction for slip	0.6
In situ stress ratio (S_{hmin}/S_V)	0.7

Finally, it is assumed that CO_2 injection increases reservoir pressure to 2000 psi. Taking account of poroelastic effects and assuming a Poisson's ratio of 0.3 for the coal, the Mohr circle moves from II to III. For this case, there is still no slip on discontinuities. However, for Poisson's ratio of 0.4, $\Delta S_{hmin} = 0.23\Delta P$, and the Mohr circle moves from II′ to III′; intersecting the criterion for slip. During repressurization more stable conditions are attained if the Poisson's ratio of the reservoir material is low.

The dip of discontinuities upon which slip would occur can be determined from the intersection of the Mohr circle with the failure criteria. The equations for the two values of β corresponding to the points of intersection are [34]

$$2\beta_1 = \pi + \varphi - \sin^{-1}[(\sigma_m/\tau_m)\sin\varphi]$$

and

$$2\beta_2 = \varphi + \sin^{-1}[(\sigma_m/\tau_m)\sin\varphi]$$

where

$$\varphi = \tan^{-1}\mu$$

$$\sigma_m = \tfrac{1}{2}(\sigma_1 + \sigma_3)$$

$$\tau_m = \tfrac{1}{2}(\sigma_1 - \sigma_3)$$

For conditions represented by the circle III′ in Figure 9, slip would occur on discontinuities with dips between 50° and 70°.

Results of these analyses are very sensitive to the in situ stress state. The risk of slip is significantly reduced as $S_{hmin}/S_V \rightarrow 1$. If the stability analysis is repeated assuming $S_{hmin}/S_V = 1$, a common assumption in reservoir simulation, then no slip would be predicted for any of the reservoir pressure conditions. However, if $S_{hmin}/S_V = 0.6$, slip is predicted even under the assumed initial reservoir pressure of 1500 psi.

Failure and slip in the overburden

So far, the discussion has focused only on the risk of failure or slip within the coal seam. However, potential leakage paths require failure in slip in the bounding rock layers as well as in the coal seam. A possible, though least likely mechanism, is the propagation of a shear failure from the coal into the bounding rock. As discussed previously, fracture propagation into the bounding rock is impeded when the coal strength is less than the strength of the bounding rock.

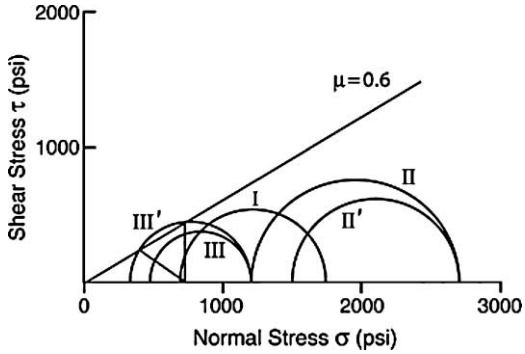

Figure 9: Mohr circles for slip on a discontinuity in a coal seam under conditions representative of the San Juan basin.

Volumetric changes in the reservoir have an important influence on displacements in the overburden. During production, there is a volumetric decrease in the reservoir due to pore pressure reduction. The amount of volumetric decrease is a function of the compressibility of the reservoir rock and its thickness. In coal there is an added component due to shrinkage from desorption of the methane. The volumetric decrease in the reservoir may cause subsidence of the overburden. On the flanks of the reservoir, bending of the overburden layers results in shear stresses which can cause failure or slip on pre-existing discontinuities. If the pore pressure distribution, and hence, volumetric deformation, in the reservoir is not uniform, shear displacements in the overburden will be introduced at places other than the flanks.

Repressurization of the reservoir may cause volumetric expansion and upward displacement, or heave, in the overburden. The effect on shear displacements is to reverse the sense of motion. Thus, shear displacement on a discontinuity can move in one direction during drawdown and reverse and move in the opposite direction during injection. An example of this is shown in Figure 10. The figure shows modeled

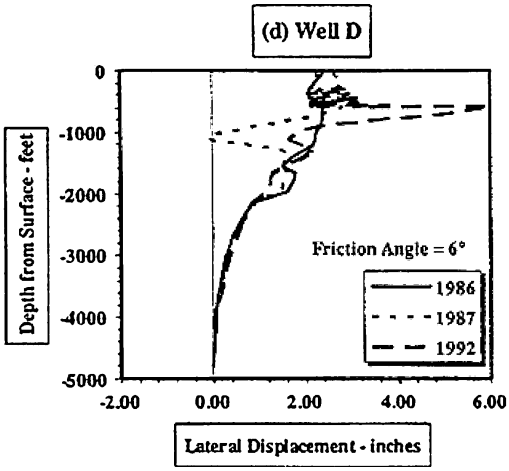

Figure 10: Numerical simulation of lateral displacement of a well in the South Belridge reservoir. Large lateral displacements at about 1000 ft depth occur due to slip on an interface with a friction angle of 6°. Lateral displacements reverse between the years of 1987 and 1992 [35].

well displacements due to shear on a weak zone in the overburden above the South Belridge oil reservoir. This reservoir has undergone pressure drawdown from production and then repressurization from aggressive water injection.

An example of the development of shear displacements near the interface between the reservoir and overburden when CO_2 is injected is shown in Figure 11. The figure shows results of a numerical simulation of injection of CO_2 from a single well into a brine-saturated layer. The shaded region in part b of the figure shows where shear stresses develop. The blue outline shows the extent of the CO_2 plume. The volumetric expansion of coal with CO_2 will have an additional component due to swelling associated with gas sorption. Experimental work indicates that CO_2 causes more volumetric changes than methane. This will further alter the distribution of volumetric expansion resulting from repressurization.

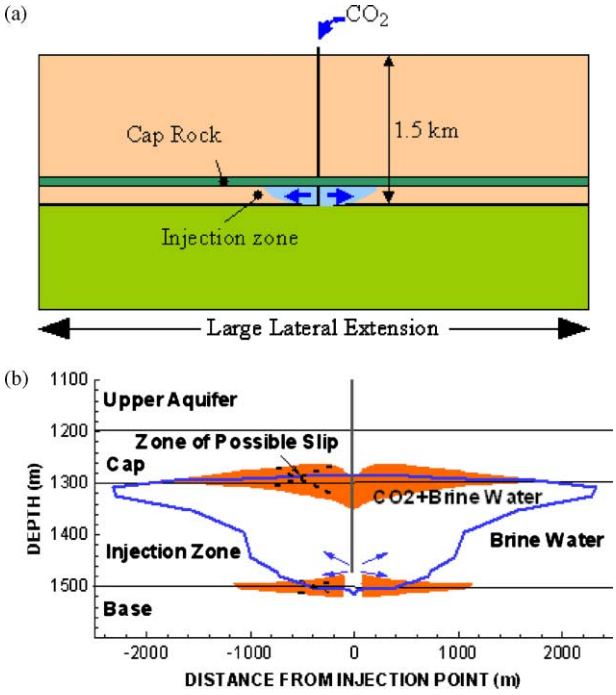

Figure 11: Results of numerical simulation of stresses and displacements due to injection of CO_2 into a brine saturated formation [36]. (a) The model. (b) Outline of plume and region where shear stresses could cause slip on discontinuities.

If a pre-existing discontinuity cuts across the coal seam, model results show that slip can occur in the overburden, outside of the region of pore pressure change. Figure 12a shows a model in which there is a pressurized region between two discontinuities ("faults") dipping at 45°. Calculations were carried out using the coupled hydrologic/geomechanical simulator TOUGH-FLAC [37]. The faults were represented by "slip lines" with a friction angle of 25°. Figure 12b shows the shear slip on the faults as a function of depth. Due to the symmetry of the problem, the sense of motion is in one direction on one fault and in the opposite direction on the other fault. It is seen that the magnitude of the slip is greatest within the region of pressure increase and tails off quickly outside the region.

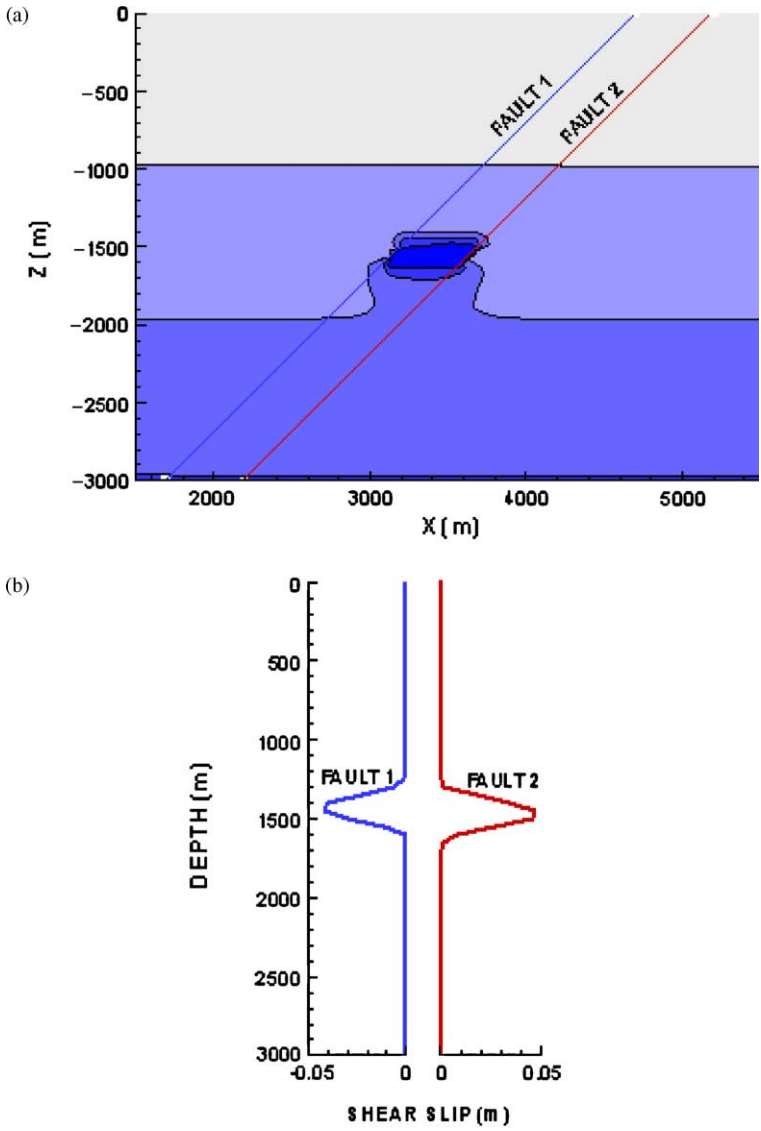

Figure 12: Numerical simulation of slip on discontinuities resulting from a pressurized region. (a) The model, showing a maximum pressure increase in the region of 2.6 times original pressure. (b) Shear slip on the faults.

Slip on pre-existing faults and other discontinuities which intersect the coal seam are viewed as a likely scenario for generation of possible leakage paths for CO_2. Numerical sensitivity studies should be performed to evaluate the effects the dip and frictional properties of faults for representative coal seam pressure changes. It is important to capture coal volumetric changes due to sorption and desorption as part of these models.

While slip on pre-existing discontinuities creates a potential leakage path, further analysis is required to evaluate whether or not fluid flow will occur in conjunction with the slip. The risk of leakage will be increased if the magnitude of the slip is on the order of bed thickness. Geologic studies of fault seals have shown that fault movement which brings sand layers into contact can lead to fluid flow across faults from higher to lower pressure sands.

The degree to which slip will increase the potential for flow along faults and discontinuities is much less well understood. Laboratory tests have shown that shearing a rock fracture in rock will increase its permeability as a result of dilatancy. Since fracture surfaces are rough, shear displacements can lead to an opening of the fracture and an increase in permeability. Less dilatancy would be expected for faults or discontinuities filled with clay gouge. The relationship between stress state, slip magnitude, fault and fracture surface geometry and changes in hydrologic properties of infilling materials is an area requiring substantial additional basic research.

Other Potential Failure Modes

The risk of methane emission is another environmental issue that must be considered during CO_2 enhanced coalbed methane production. Methane is the second most important greenhouse gas, responsible for about 15% of the greenhouse gas buildup in the atmosphere to date (Greengas.htm). Molecule for molecule, methane traps about 27 times more heat than CO_2.

Ideally, the majority of injected CO_2 will be trapped by adsorption onto the surface of coal matrices. However, CO_2 retention in a coalbed is largely dictated by how effectively the injected CO_2 contacts and interacts with the coalbed over the project lifetime. As observed in the Tiffany field, the early N_2 breakthrough and high N_2 cut indicated that the injected N_2 may only contact a small portion of the total available pay [13,42] (Chapter 15, this volume).

Coalbed water, whose salinity varies from fairly fresh to very saline, is a potential water resource for domestic, irrigation, industrial, mining, and thermoelectric use. In 1990, about 48 million gallons per day (MGD) of saline ground water was utilized in the United States as a source of public water supply, mostly for thermoelectric power. This represents a 28% increase since 1987 and a 178% increase since 1985. The potential future usage of coalbed water, therefore, must be taken into account in the selection of a coalbed CO_2 storage site.

Given the complex and unique nature of storing CO_2 in coalbeds, risks exist both during and after the injection of CO_2. Besides the risk scenarios common to other geological formations, storing CO_2 in coalbeds has five additional pitfalls that should be assessed carefully:

- insufficient CO_2–coal contact volume due to coalbed heterogeneity;
- injectivity loss due to coal swelling caused by CO_2 adsorption;
- CO_2 and methane leakage through pre-existing faults and discontinuities;
- CO_2 and methane seepage through outcrops; and
- CO_2 and methane desorption due to potential future coalbed water extraction.

Table 2 summarized the most likely failure modes that pertain to the operation of CO_2 storage in coalbeds. Along with the failure modes, their potential initiators and consequences are provided. The duration of a failure mode is indicated by short term (S), or long term (L), or both.

PROBABILISTIC RISK ASSESSMENT METHODOLOGY

Conceptually, a risk assessment methodology should include four major elements: hazard identification, event and failure quantification, predictive modeling, and risk characterization. The hazards of CO_2 exposure are well known and described in Benson et al. [39] and Chapter 27 of this volume. Similarly the hazards of methane releases are well known [7–12,38].

TABLE 2
SUMMARY OF FAILURE MODES PERTAINING TO CO_2 STORAGE IN COALBEDS

Failure modes	Event initiators	Consequences	Short/ long term
CO_2 pipeline failure	Corrosion, manufacturer's defects, earthquake, sabotage	Short-term release of concentrated CO_2 into atmosphere, human safety and health hazard	S
Compressor failure	Corrosion, improper maintenance, manufacturer's defects	Interruption of CO_2 injection	S
Well string failure (surface casing, intermediate casing, tubing, etc.)	Corrosion, manufacturer's defects	CO_2 migration out of zone, CO_2 migration into meteoric water, absolute open flow (AOF), human safety and health hazard	S&L
Cement failure	Corrosion, poor cement bond	CO_2 migration out of zone, CO_2 migration into meteoric water, AOF, human safety and health hazard	S&L
Seal failure	CO_2/H_2O/rock interactions, in situ stress by coal swelling, over pressurization	CO_2 migration out of zone, CO_2 migration into meteoric water, reduced sequestration capacity, diminished recovery, catastrophic CO_2 release into atmosphere, human safety and health hazard	S&L
Fracture extension within zone or into overburden	Injection above parting pressure, hydraulic fracturing, earthquake	Long-term CO_2 release into atmosphere, CO_2 migration into meteoric water, asset degradation, AOF, human safety and health hazard	S&L
Injectivity loss	Coal swelling caused by CO_2 adsorption	Lower-than-planned injection rate, asset degradation, early project termination	S
Insufficient storage capacity	Reservoir heterogeneity	Early project termination, asset degradation	S
Insufficient methane ecovery	Reservoir heterogeneity	Early project termination, asset degradation	S
Methane and CO_2 seepage through outcrops	Methane and CO_2 release paths leading to outcrops	Long-term methane and CO_2 release into atmosphere, human safety and health hazard	S&L
Methane and CO_2 seepage through out-of-area abandoned wells	Methane and CO_2 migration out of sequestration area, poor cement bond and wellbore integrity	Long-term methane and CO_2 release into atmosphere, methane and CO_2 migration into meteoric water, human safety and health hazard	S&L

(*continued*)

TABLE 2
CONTINUED

Failure modes	Event initiators	Consequences	Short/ long term
Seal penetration	Future oil and gas drilling activities into underlying reservoirs	Methane and CO_2 migration out of zone, methane and CO_2 migration into meteoric water, catastrophic methane and CO_2 release into atmosphere, human safety and health hazard	S&L
Annular cement failure in converting old wells to CO_2 injection wells	Deteriorated or missing cement in the annular space between the casing and the rock	CO_2 leakage into overlying formations from injection wellbore	S
Overlying strata displacement	Open cavity completion	Generating fractures and CO_2 leakage paths in overburden	S&L
Coal seam slip on pre-existing discontinuities	Tectonic activity, earthquake, formation pore pressure above pre-developed level due to CO_2 injection	Potential slip and methane and CO_2 leakage paths in the bounding rock layers, catastrophic methane and CO_2 release into atmosphere, human safety and health hazard	S&L
Hydrostatic pressure drop down in coal seam	Declined water table caused by coalbed water extraction, coalbed water leakage due to underlying strata displacements	Methane and CO_2 desorption from coal matrix, catastrophic methane and CO_2 seepage from outcrops and pre-existing leakage paths, human safety and health hazard	L

Identifying and quantifying potential failure modes (event and failure quantification) at a CO_2 storage site, during and after the injection operation, is an essential part of any risk assessment. In general, any potential breach of storage integrity and normal operation can be regarded as a potential failure mode. As illustrated in Figure 13, a failure can be caused by reservoir properties and natural events, but may also be caused by engineering failures. We use the following set of questions as the guideline in identifying potential failure modes:

- What can go wrong? What causes the failure?
- What is the likelihood of the failure happening?
- How much CO_2 (and methane) could be released?
- What are the consequences?
- What is the remediation cost if the failure is reparable?

Finding credible answers to these questions is often not easy. Reservoir simulation and predictive modeling will be required to estimate the quantity and rate of unintended CO_2 and methane release. In the final step, risk characterization, quantitative estimates of methane and CO_2 leakage will be compared to a set of criteria that define, for example, acceptable rates of leakage and CO_2 exposure.

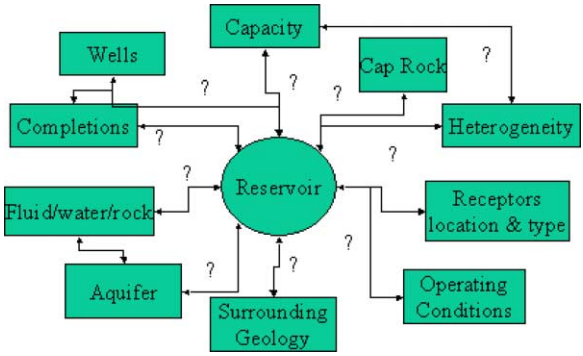

Figure 13: Examples of potential failure modes.

As discussed in Introduction, uncertainties are inherent in almost every aspect of the operation during and after the project lifetime. Consequently, a risk assessment process must be designed as a dynamic system capable of quickly redoing risk assessments when additional or updated data become available. In addition, failure modes can interact or cascade with one another. The consistency, transparency, and correctness in inference logic of such a risk assessment system must be validated. The traditional decision-tree approach, which is usually effective for simple problems, is inadequate in handling large, complex, and dynamic systems.

To make the risk assessment process rigorous and transparent, a mathematical model specifically designed for probabilistic risk assessment was developed. The guidelines for model development were

- generality and transparency;
- designed for implementation on a relational database;
- inference rules can be converted to and verified by set operations; and
- quantified indicators as model outputs.

The inference logic of this model is based on set theory, which is superior to the traditional decision-tree based inference logic, in terms of flexibility, generality, capability in dealing with uncertainties and handling large, complex problems, such as cascading phenomena. The model is also applicable for the risk assessment of CO_2 storage in other geological formations such as oil and gas reservoirs. For simplification, only CO_2 leakage is considered in the model configuration but methane leakage can be modeled similarly.

Mathematical Model

Model constituents

To create a rigorous inference system, various factors and terminologies from a real-world risk scenario must be abstracted to a limited set of functional constituents. In this model, six functional constituents have been identified. They are initiators, processes, failure modes, consequences (effects), indicators, and inference queries. In a database application, each constituent will be implemented as a database table. The six sets of constituents are symbolically defined by

(1) $I = \{i_1, i_2, i_3, \ldots\}$, Initiators.
(2) $P = \{p_1, p_2, p_3, \ldots\}$, Processes.
(3) $M = \{m_1, m_2, m_3, \ldots\}$, Failure Modes.
(4) $C = \{c_1, c_2, c_3, \ldots\}$, Consequences (effects).
(5) $D = \{d_1, d_2, d_3, \ldots\}$, Indicators.
(6) $Q = \{q_1, q_2, q_3, \ldots\}$, Inference queries.

The concept of a failure mode was already discussed and defined. Any cause leading to a failure mode is regarded as an initiator. Any effect, usually an adverse effect, is called a consequence. In cascading phenomena, a consequence of one failure mode can be the initiator of other failure modes. The fate and transport of CO_2 is represented by a set of processes. A process can represent a planned CO_2 path or an unintended CO_2 release path. To make the risk characterization transparent and meaningful, results from a risk assessment need to be organized and presented by meaningful indicators. Generally, indicators can be classified into two groups: descriptive indicators and performance indicators. Descriptive indicators provide mainly statistical information, such as averages, maxima, minima, and risk profiles while performance indicators compare different scenarios. An example of a performance indicator is the difference between the current CO_2 in-place (a specified scenario) and the maximum capacity (the base scenario). Other examples of indicators are activated initiators and their likelihood, affected processes (failure modes), consequences and associated severity scales, process tree, initiator–process–consequence diagram, consequence–process–initiator diagram, initiator–consequence diagram, overall risk index, sensitivity of initiators to the overall risk, and sensitivity of consequences to the overall risk. In some cases, additional information and criteria are required in the determination of certain initiators and consequences or in a decision-making process. These supplement information and criteria will be stored in the Inference Query table.

Inference rules

In the next step, relationships and connections between the constituents are converted to set operations, or so-called inference rules. Inference rules can be developed based on expert judgment, results of mathematical models or from statistical analysis of data from related experience. The quality of the information contained in the inference rules dictates the quality of the risk assessment. Over time, the quality of the information contained in the inference rules will improve if the experience from geologic storage projects is incorporated. Similarly, models are expected to improve as real-world data sets are used to calibrate and verify them.

For assessing underground CO_2 storage, inference rules can be categorized into seven different types.

(1) $P \Leftarrow \vec{F}_{\mathrm{P}}(I)$, identify processes affected by each initiator.
(2) $M \Leftarrow \vec{F}_{\mathrm{M}}(P)$, define failure modes associated with each process.
(3) $C \Leftarrow \vec{F}_{\mathrm{C}}(P, M)$, identify consequences if a failure mode occurs.
(4) $I \Leftarrow \vec{F}_{\mathrm{I}}(C)$, identify cascading effects.
(5) $D \Leftarrow \vec{F}_{\mathrm{D}}(I, P, M, C)$, dynamically calculate and reevaluate indicators.
(6) $I \Leftarrow \vec{F}_{\mathrm{I}}(Q)$, indirectly identify initiators.
(7) $C \Leftarrow \vec{F}_{\mathrm{C}}(Q)$, indirectly identify consequences.

In a database application, inference rules of the same type will be implemented in one database table. Because processes are associated directly with CO_2 transport or release paths, the natural cascading flow path of CO_2 can be used in defining how processes are linked one to another. As a part of the process properties stored in the process table, the description of the connections to up-stream and down-stream processes are required information that will later be used in calculating the likelihood of cascaded CO_2 releases.

It is worth pointing out that, in general, decision-tree based rules can be converted to set operations as demonstrated in the following example (see Figure 14). A simple decision tree for identifying initiators consists of three Questions (criteria) and four possible Initiators (answers). As shown in Figure 14a relational table between the set of Questions and the set of Initiators is generated in which each column represents a possible decision route.

The relational table implies two sets of inference rules: (1) if a question is known, then it indicates possible initiators or (2) if an initiator occurs, then it gives the answers to the questions. In comparison, an inference rule can be represented by a route of a decision tree or equivalently by set operations as demonstrated in the following example.

Decision Tree: If Q_1 true and Q_2 false then I_2
Set Operation: $\{I_1, I_2\} \cap \{I_2\} = I_2$

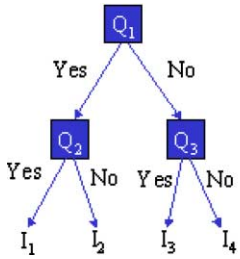

	I_1	I_2	I_3	I_4
Q_1	Yes	Yes	No	No
Q_2	Yes	No	NA	NA
Q_3	NA	NA	Yes	No

Figure 14: The conversion between a simple decision tree and its relational table.

Severity scale of consequences

Quantifying the severity of a consequence is probably the most difficult task in risk assessment. We suggest using a numerical scaling system based on the set of criteria shown in Table 3. Ranking risks by standardized criterion such as these has already been used for other complex systems [40].

In addition to CO_2 release rate and remediate cost, other criteria in risk assessment may include adverse effect to human health, adverse effect to animals, potentiality in regulation breach, duration, cascading effect, undetectability, uncontrollability, and irreversibility. After the criteria are accepted, a numerical severity scale, for example between 0 and 1, will be defined according to the effective impact of a consequence based on expert knowledge, statistical data, and regulations. In practice, the average value of all severity scales can be used to indicate the overall severity scale of a consequence. The overall severity scale could also include a weighting factor that recognizes that not all factors are equally important (e.g. risk to human life may be weighted more strongly than undetectability).

$$\text{Average Severity Scale} = \frac{\sum_i S_i}{\text{Number of Criteria}}$$

TABLE 3
EXAMPLES OF CRITERIA FOR THE SEVERITY ASSESSMENT OF CONSEQUENCES

Criterion	**Severity scale (0–1)**
Adverse effect to human health	S_1
Adverse effect to animals	S_2
Potentiality of violating regulations	S_3
Duration	S_4
Cascading effect	S_5
Undetectability	S_6
Uncontrollability	S_7
Irreversibility	S_8

Likelihood of failures

For a given failure mode, M, we use *LIKELIHOOD(M)* to indicate the failure likelihood of M (*LIKELIHOOD(M)* ranges from 0 to 1). Let P be the process associated with the failure mode M. Without losing generality, we assume that the failure could be caused by each of n identified initiators, $\{I_1, I_2, \ldots, I_n\}$. The failure likelihood caused by initiator I_i alone is given by $LIKELIHOOD(I_i)$, $i = 1–n$.

The effective failure likelihood caused by the combined effects of the n initiators can be calculated from the following iterative procedure.

$$LIKELIHOOD(\{I_1, I_2, \ldots, I_i\})] = LIKELIHOOD(I_i) + LIKELIHOOD(\{I_1, I_2, \ldots, I_{i-1}\}) - LIKELIHOOD(I_i) * LIKELIHOOD(\{I_1, I_2, \ldots, I_{i-1}\}), i = 2\text{–}n.$$

We define the failure likelihood of M as

$$LIKELIHOOD(M) = LIKELIHOOD(P) * LIKELIHOOD(\{I_1, I_2, \ldots, I_n\})$$

where *LIKELIHOOD(P)* is the likelihood of CO_2 existence in process P and is defined by

$$LIKELIHOOD(P) = \begin{cases} 1, & \text{if } P \text{ is a planned } CO_2 \text{ path} \\ \prod_k LIKELIHOOD(M_k), & \text{otherwise} \end{cases}$$

In the above definition, M_k represents a preceding failure mode on the cascading CO_2 release path to the process P and *LIKELIHOOD(Mk)* is its failure likelihood.

Rate, cost, and effective severities

In probabilistic risk assessment, the failure likelihood of a failure mode is considered to be equally important as other factors in the evaluation of effective severities.

Let $Rate^*$ and $Cost^*$ be the estimated CO_2 release rate and remediation cost in the case where 100% failure occurs to the failure mode, M. After the failure likelihood of M is obtained, the effective CO_2 release rate can be evaluated by

$$Rate = Rate^* * LIKELIHOOD(M)$$

and the effective reparable cost of the failure mode can be estimated by

$$Cost = Cost^* * LIKELIHOOD(M)$$

For each of the identified consequences of M, its effective severity scale can then be evaluated by the geometric average of its severity scale and the failure likelihood of M,

$$\sqrt{(Severity\ \ Scale\ \ of\ \ Consequence) * LIKELIHOOD(M)}$$

Risk scenario simulator

A relational database, such as MS Access, is capable not only of managing large datasets but can also perform complex dataset operations. Because the inference rules of the model are represented as set operations, a database application of the model can entirely be coded by database language, which is referred to as the risk scenario simulator. A scenario simulation will consist of the following steps: (1) activating selected initiators, (2) identifying affected processes, (3) calculating the failure likelihood of each failure mode, (4) identifying their consequences, (5) estimating the effective CO_2 release rates, reparable costs, and the effective severity scales of consequences, and (6) repeating steps (1)–(5) if new initiators have been invoked by resulting consequences (cascading effects). Practically, once initiators are manually activated in step 1, the rest of steps and computational works can be performed by pre-stored procedures. A prototype application has been developed and will be discussed in the following section.

RESULTS AND DISCUSSION

Leakage Quantification

Identifying potential leakage pathways and estimating leakage flux are the two basic tasks for leakage evaluation. The severity of a leakage is directly related to the leakage rate. Structural geology and monitoring data at historic seep sites provide a useful indication of existing leakage paths and flux intensity. Reservoir modeling is an essential tool for quantitative predictions of CO_2 and methane transport in

sedimentary strata. The water–gas transport through the coal cleat system is normally described by Darcy's law for two-phase flow, which is applied by most current CBM simulators and is capable to predict CO_2 and methane seepage rates at outcrops. In contrast, modeling vertical seepage is much more difficult. Variations in overlying stratigraghic column and formation structures complicate the model settings. Unsaturated zones and fracture networks may cause further uncertainties in flow regimes. In fact, the majority of vertical seepage flux may largely be controlled by fracture networks [14,41–44].

Once gas seeps into fractures, the buoyancy force drives gas bubbles migrating upward to the surface. Brown [41] analyzed gas flow in fractures and proposed four mechanisms for gas migration in fractures. They are (1) continuous-phase gas migrating in fractures, (2) bubble ascent without wall or concentration effects (Stokes' law), (3) maximum velocity of isolated bubble ascent in fractures, and (4) steady ascent of bubbly water in a vertical fracture having infinitesimal bubble size and 18% gas concentration. Figure 15 shows the calculated gas migration velocities along a fracture for the four different mechanisms. By comparing reported seepage velocities (in the order of 100–10,000 m/yr), Brown [41] concluded that single-phase gas flow in fractures having half widths from 0.1 to 2 μm can be responsible for buoyancy-driven flow at rates equal to the range of reported seepage velocity (Figure 15).

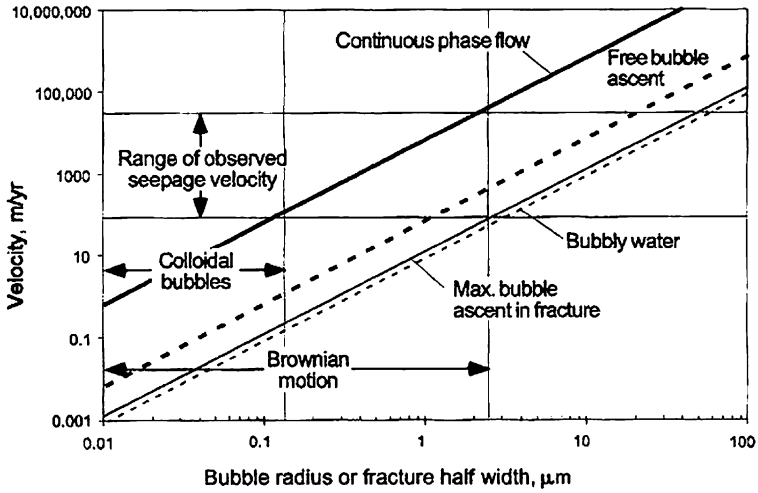

Figure 15: Comparison of calculated migration velocities for the different mechanisms and observed seepage velocities [41].

Leakage in wellbores can be detected by tracer tests, image and casing bond logs, and Bradenhead (casing) pressure tests. Bradenhead (casing) pressure monitoring is routinely required for gas wells in the San Juan Basin. A threshold pressure of 25 psig (2 psig in the critical areas) was established by the BLM in 1991 [10]. Therefore, the likelihood of gas leakage in the annular space can be directly evaluated according to the measured Bradenhead pressure, as shown in Figure 16.

In general, a failure mode's failure likelihood caused by an identified initiator can usually be represented as a function (cumulative probability distribution) of relevant parameters, such as simulated leakage flux, injection pressure, fracture density, and statistical data. Similarly, the severity scale of a consequence can be determined by its measurable parameters. In Figure 17, the severity scales to human safety and health are assessed by the CO_2 release rate and the distance to the source point.

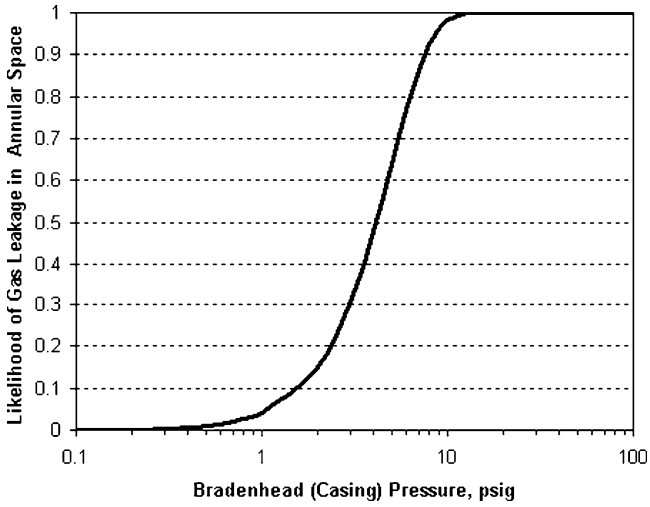

Figure 16: Bradenhead (casing) as an indicator of gas leakage in the annular space.

Software Tool Development

To demonstrate the applicability of the model, Microsoft Access was used as a platform to develop a prototype application. Complying with the major steps of the assessment procedure, the application consists of several modules that reside in the database as functional combinations of tables, forms, and stored procedures. For a new project, after risk scenarios have been identified, a user can use the main user interface and its pop-up interfaces to define processes, failure modes, initiators, and consequences.

Once the risk scenarios are defined and entered into the database, quantifying and tuning each failure mode is the main task performed via the Failure Mode form interface (see Figure 18). In the top-left corner of the form, there is a drop-down list for the selection of any defined failure modes. When a failure mode is selected, all the data and computations will be associated with the selected failure mode. By changing settings, for example, activating/deactivating initiators and consequences, changing likelihood values, changing maximum cost, and changing maximum CO_2 release rate, one can quickly perform risk quantification for different risk scenarios. The results are dynamically and visually presented by the severity matrix. After each failure mode has been properly tuned, one can simultaneously run all failure modes together to see the interaction and cascading effects between the failure modes.

Scenario simulation vs. Monte Carlo simulation

When the UPDATE button on the Failure Mode form is clicked, only a single scenario simulation will be performed. In addition, a built-in Monte Carlo simulation procedure is also provided. To perform a Monte Carlo simulation, the number of seeds (runs) has to be selected first from the drop-down list (Figure 18). By clicking the Monte Carlo simulation button, the Monte Carlo simulation will be performed and the results will be saved in the table of Monte Carlo-Failure Mode. The difference between a single scenario simulation and the Monte Carlo simulation is in how to select the failure likelihood of the initiators. In a single scenario simulation run, we use

$$I_i \text{ with } LIKELIHOOD(I_i),\ i = 1\text{–}N$$

While for a series of Monte Carlo runs, we use

$$I_i \text{ with } LIKELIHOOD_{MC}(I_i),\ i = 1\text{–}N,$$

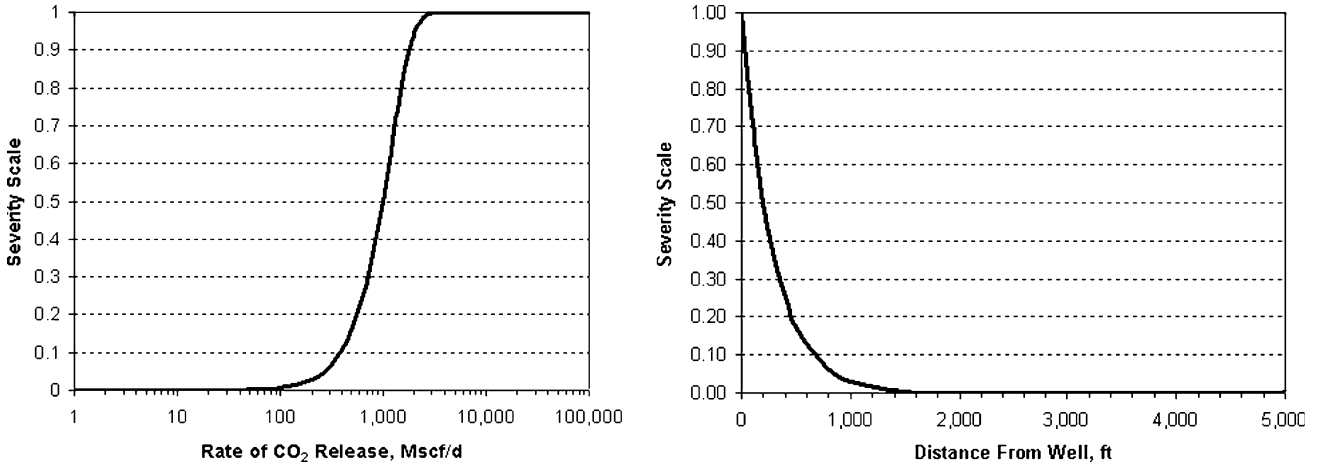

Figure 17: Rate effect (left) and distance effect (right) of point source CO_2 release into atmosphere on severity of human safety and health hazard.

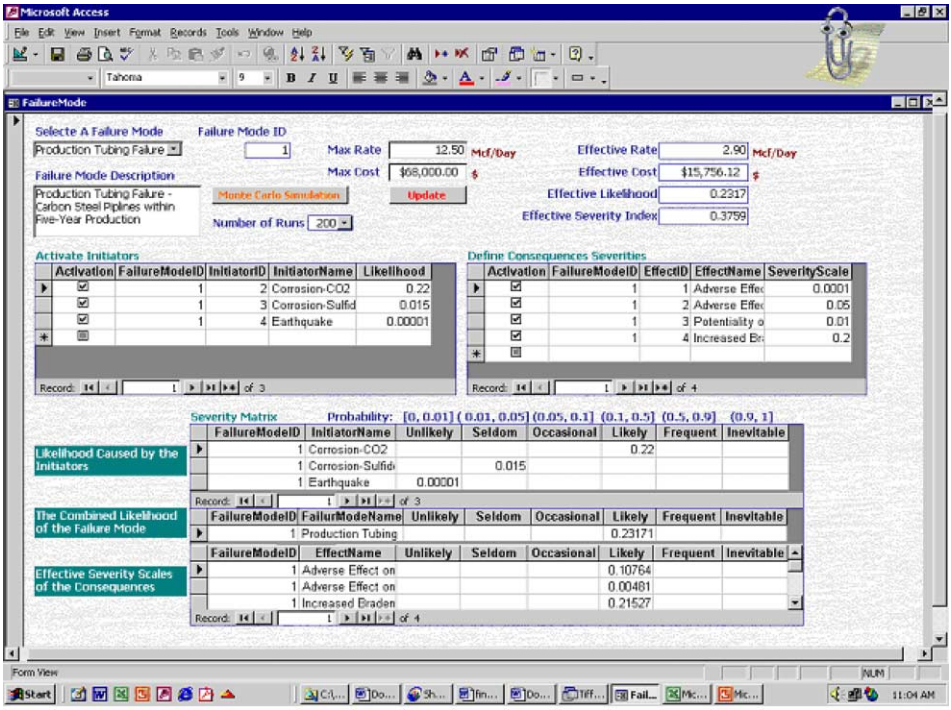

Figure 18: The user interface of the Failure Mode form.

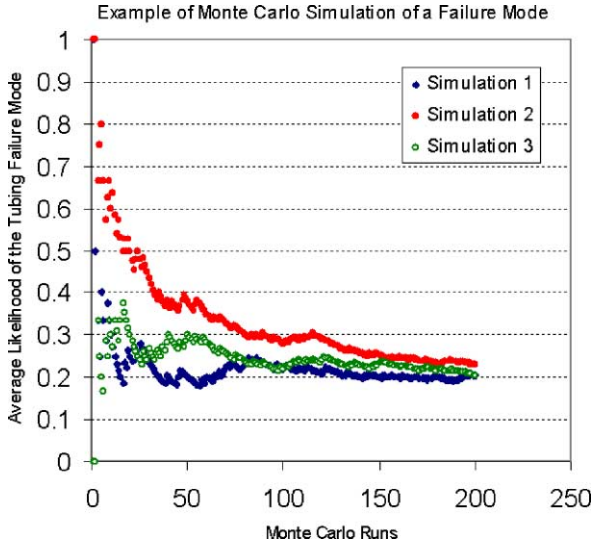

Figure 19: Average likelihood vs. number of Monte Carlo runs.

where

$$LIKELIHOOD_{MC}(I_i) = \begin{cases} 0 & \text{if } LIKELIHOOD(I_i) < Random() \leq 1 \\ 1 & \text{if } 0 \leq Random(\ ) \leq LIKELIHOOD(I_i) \end{cases}$$

To prevent over-sized tables, the Monte Carlo-Failure Mode table only keeps the results from the most recent run. Figure 19 shows the plot of the average likelihood versus the number of Monte Carlo runs where 200 seeds (runs) were used for all three Monte Carlo simulations. In this example of production tubing failure, three initiators were activated, Corrosion-CO_2, Corrosion-Sulfide, and Earthquake, with likelihood of 0.22, 0.015, and 0.00001, respectively for a 5-year production period. After 200 runs, the average likelihood from the Monte Carlo simulations all approach the combined likelihood of 0.23171.

CONCLUSIONS

Geomechanical processes lead to risks of developing leakage pathways for CO_2 and methane at each step in a coalbed methane project for methane production and eventual CO_2 storage. Though each of the risks identified in this study need to be evaluated for specific sites, the following general conclusions have been drawn from this review:

- Conventional techniques are available to minimize risk of leaks in new well construction though additional study should be devoted to establish best practices for the height of cement behind production casing; risk of leakage is higher for old wells converted to injectors.
- Risks of leakage are much higher for open cavity completions than for cased well completions.
- Coal properties and available technology should minimize the risk that hydrofractures, used as part of completion, will grow out of interval; techniques to monitor fracture height need further development.
- The processes of depressurization during dewatering and methane production, followed by repressurization during CO_2 injection, lead to risks of leakage path formation by failure of the coal and slip on discontinuities in the coal and overburden.
- The most likely mechanism for leakage path formation is slip on pre-existing discontinuities which cut across the coal seam. Sensitivity studies need to be performed to better evaluate this risk.
- Relationships between the amount of slip and the increase in flow (if any) along a discontinuity need to be developed.

The risk assessment methodology proposed in this study includes four major elements: hazard identification, event and failure quantification, predictive modeling, and risk characterization. The central part of the methodology is a mathematical model, wherein potential CO_2 and methane leakage pathways are defined by failure modes. The results from this work are summarized as follows:

- A mathematical model for probabilistic risk assessment was developed. The model consists of six functional constituents, initiators, processes, failure modes, consequences (effects), indicators, and inference queries. The model was designed to implement on a relational database.
- For assessing the risks of CO_2 storage in geological formations, inference rules can generally be categorized into seven different types. The inference logic of this model is based on set theory, which is superior to the traditional decision-tree based inference logic, in terms of flexibility, generality, capability in dealing with uncertainties and handling large, complex problems, such as cascading phenomena.
- The mathematical model provides a logic and computational basis for a risk-based scenario simulator.
- To demonstrate the applicability of the mathematical model, a prototype application was developed in Microsoft Access. The application consists of several modules that reside in the database as functional combinations of tables, forms, and stored procedures. An intuitive main user interface and its pop-up interfaces are created to facilitate the data input and risk assessment process. The application can perform both scenario simulations and Monte Carlo simulations.
- In addition to the risk scenarios common to other geological formations, storing CO_2 in coalbeds may face other pitfalls. The likely risks pertaining to CO_2 injection and storage in coalbeds include: insufficient CO_2–coal contact volume due to coalbed heterogeneity, injectivity loss due to coal swelling

caused by CO_2 adsorption, CO_2 and methane leakage through pre-existing faults and discontinuities, CO_2 and methane leakage through outcrops. In the long term, CO_2 and methane desorption caused by potential coalbed water extraction after the project lifetime is also a concern.

ACKNOWLEDGEMENTS

We are grateful to Daryl Erickson of BP America Inc. for providing helpful insights and the Tiffany field data. This work was supported in part by a Cooperative Research and Development Agreement (CRADA) between BP America Inc., as part of the CO_2 Capture Project (CCP) of the Joint Industry Program (JIP), and the US Department of Energy (DOE) through the National Energy Technologies Laboratory (NETL) under contract DE-AC07-99ID13727.

REFERENCES

1. S.R. Reeves, Enhanced CBM recovery, coalbed CO_2 storage assessed, *Oil Gas J.* **101** (27) (2003) 14.
2. D. Erickson, Overview of ECBM Commercial Demonstration Pilot at Tiffany Unit, Internal Report, BP America, 2002, October.
3. K.A.M. Gasem, R.L. Robinson Jr., S.R. Reeves, Adsorption of Pure Methane, Nitrogen, and Carbon Dioxide and Their Mixtures on San Juan Basin Coal, DOE Topical Report, 2002, May.
4. S.R. Reeves, Geologic Storage of CO2 in Deep, Unmineable Coalbeds: An Integrated Research and Commercial-Scale Field Demonstration Project, SPE 71749, Proceedings of the SPE Annual Technical Conference and Exhibition, New Orleans, September 30–October 3, 2001.
5. S.R. Reeves, C. Clarkson, D. Erickson, Selected Field for ECBM Recovery and CO2 Storage in Coal based on Experience Gained at the Allison and Tiffany Units, San Juan Basin, DOE Topical Report DE-FC26-00NT40924, September 30, 2002.
6. S. Reeves, A. Taillefert, L. Pekot, C. Clarkson, The Allison Unit CO_2—ECBM Pilot: A Reservoir Modeling Study, DOE Topical Report, 2003, February.
7. Amoco, Pine River Fruitland Coal Outcrop Investigation: Southern Rockies Business Unit, Amoco Production Company, Denver, CO, 1994.
8. Advanced Resources International Inc., Gas seepage in the Pine River Area, Colorado, prepared for the Geological and Reservoir Engineering Subcommittee of the Pine River Fruitland Coal Investigative Team, November 1994.
9. P. Oldaker, Monitoring data review, Pine River ranches, prepared for Colorado Oil and Gas Conservation Commission and Amoco Production Company, USA, 1999.
10. Bureau of Land Management (BLM), San Juan Field Office, Coalbed Methane Development in The Northern San Juan Basin of Colorado, December 1999.
11. Questa Engineering Corporation, The 3M coalbed methane reservoir model, Prepared for the Southern Ute Indian Tribe, Ignacio, Colorado, the Colorado Oil and Gas Conservation Commission, Denver, Colorado, and the Bureau of Land Management, Durango, Colorado, May 26, 2000.
12. L.L. Wray, Late Cretaceous fruitland formation geologic mapping, outcrop measured sections, and subsurface stratigraphic cross sections, Northern La Plata County, Colorado, Colorado Geological Survey Open File Report 00-18, Denver, Colorado, 2000.
13. S. Wo, J.T. Liang, Simulation assessment of N_2/CO_2 contact volume in coal and its impact on outcrop seepage in N_2/CO_2 injection for enhanced coalbed methane recovery, The 14th Improved Oil Recovery Symposium, Tulsa, Oklahoma, April 17–21, 2004.
14. C.R. Nelson, Geologic controls on effective cleat porosity variation in San Juan basin Fruitland Formation coalbed reservoirs, Tuscaloosa, Alabama, Proceedings, International Coalbed Methane Symposium, Paper, 108, 2001, pp. 11–19.
15. K. Ben-Naceur, Modeling of hydraulic fracture, *Reservoir Stimulation* (1989) 3-1–3-31.
16. B. Atkinson, P. Meredith, Experimental fracture mechanics data for rocks and minerals, *Fracture Mechanics of Rock* (1987) 477.
17. D. Murray, 1993, Coalbed methane reservoir evaluation and completion technology. Atlas of Major Rocky Mountain Gas Reservoirs, New Mexico Bureau of Mines and Mineral Resources, pp. 88–189, 1971.

18. U. Ahmed, Fracture-height predictions and post-treatment measurements, *Reservoir Stimulation* (1989) 10-1–10-3.
19. U. Ahmed, B.M. Newberry, D.E. Cannon, Hydraulic fracture treatment design of wells with multiple zones, SPE 13857, 1985.
20. J.A. Anderson, C.M. Pearson, A.S. Abou-Sayed, G.D. Myers, Determination of fracture height by spectral gamma log analysis. SPE 15439, Proceedings of 61th Annual Technical Conference, New Orleans, LA, 1986.
21. K. Nolte, M. Economides, Fracturing diagnosis using pressure analysis, *Reservoir Stimulation* (1989) 7-1–7-34.
22. D. Bland, Coalbed methane from the Fruitland Formation, San Juan Basin, New Mexico, North Mexico Geological Society 43rd Conference, 1992.
23. H. Poulos, E. Davis, Elastic Solutions for Soil and Rock Mechanics, Wiley, New York, 1974, p. 237.
24. K. Terzaghi, F.E. Richart, Stresses in rock about cavities, *Geotechnique* **3** (1952) 57–90.
25. C.M. Gibson-Poole, S.C. Lang, J.E. Streit, G.M. Kraishan, R.R. Hillis, Assessing a basin's potential for geological storage of carbon dioxide: an example from the Mesozoic of the Petrel Sub-basin, NW Australia. Presented at Proceedings of the Petroleum Exploration Society of Australia Symposium, Perth, Western Australia, 2002.
26. M.A. Addis, Reservoir depletion and its effect on wellbore stability evaluation, *Int. J. Rock Mech. Mining Sci.* **34** (3–4) (1997a) 423.
27. M.A. Addis, The stress-depletion response of reservoirs. SPE 38720, Proceedings of 72nd SPE Annual Technical conference and Exhibition, San Antonio, TX, 1997b.
28. L.W. Teufel, D.W. Rhett, H.E. Farrell, Effect of reservoir depletion and pore pressure drawdown on in situ stress and deformation in the Ekofisk field, North Sea, Proceedings of 32nd US Rock Mechanics Symposium, Norman, OK, 1991, pp. 63–72.
29. J.E. Streit, R.R. Hillis, Estimating fluid pressures that can induce reservoir failure during hydrocarbon depletion. Presented at SPE 78226. SPE/ISRM Rock Mechanics Conference, Irving, TX, 2002.
30. Y. Touloukian, W. Judd, R. Roy, Physical Properties of Rocks and Minerals, McGraw-Hill, New York, 1981, pp. 132–144.
31. M.A. Addis, X. Choi, J. Cumming, The influence of the reservoir stress-depletion response on the lifetime considerations of well completion design. SPE 47210, Proceedings of SPE/ISRM, Trodheim, Norway, 1998.
32. P. Peska, M.D. Zoback, Compressive and tensile failure of inclined well bores and determination of in situ stress and rock strength, *J. Geophys. Res.* **100** (1995) 12791–12811.
33. S.A.F. Murrell, The strength of coal in triaxial compression. Presented at Proceedings of Conference Mechanical Properties Non-Metallic Brittle Materials, Butterworths, London, England, 1958.
34. J.L. Jaeger, N.G.W. Cook, Fundamentals of Rock Mechanics, Chapman & Hall Ltd. and Science Paperback, 1971, p. 67.
35. L.B. Hilbert, J.T. Fredrick, M.S. Bruno, G.L. Deitrich, P.E. de Roufflignae, Two dimensional nonlinear finite element analysis of well damage due to reservoir compaction, well to well interactions and localization, *Proceedings of Second North American Rock Mechanics Symposium, Montreal, Balkema* **2** (1996) 1863–1870.
36. J. Rutqvist, C-F. Tsang, TOUGH-FLAC: A numerical simulator for analysis of coupled thermal hydrologic mechanical processes in fractured and porous geological media under multiphase flow conditions, TOUGH Symposium, Berkeley, CA, 2003.
37. J. Rutqvist, Y.-S. Wu, C-F. Tsang, G. Bodvarsson, A modeling approach for analysis of coupled multi-phase fluid flow, heat transfer, and deformation in fractured porous rock, *Int. J. Rock Mech. Mining Sci.* **39** (2002) 429–442.
38. R.W. Klusman, Evaluation of leakage potential from a carbon dioxide EOR/storage project, *Energy Conversion Manage.* **44** (2003) 1921–1940.
39. S.M. Benson, R. Hepple, J. Apps, C.-F. Tsang, Lessons Learned from Natural and Industrial Analogues for Storage of Carbon Dioxide in Deep Geological Formations, LBNL-51170, 2003.
40. Y.Y. Haimes, S. Kaplan, J.H. Lambert, Risk filtering, ranking, and management framework using hierarchical holographic modeling, *Risk Analysis* **22** (2) (2002) 000.
41. A. Brown, Evaluation of possible gas microseepage mechanisms, *AAPG Bulletin* **85** (11) (2000) 1775–1789.

42. K.T. Raterman, Assessing Reservoir Heterogeneity from a Single Well Injection Test, Internal Report, Amoco Production Company, Denver, CO, 1996.
43. C.M. Tremain, E. S, N.H. Laubach, I.I.I. Whitehead, Fracture (cleat) patterns in Upper Cretaceous Fruitland Formation coal seams, San Juan basin, in: W.B. Ayers Jr., W.R. Kaiser (Eds.), Coalbed Methane in the Upper Cretaceous Fruitland Formation, San Juan basin, New Mexico and Colorado, Bulletin, vol. 146, New Mexico Bureau of Mines and Mineral Resources, 1994, pp. 87–102.
44. J.C. Pashin, R.H. Groshong Jr., R.E. Carroll, Enhanced Coalbed Methane Recovery Through Storage of Carbon Dioxide: Potential for a Market-Based Environmental Solution in the Black Warrior Basin of Alabama, Tuscaloosa, AL, 2003.

This page is intentionally left blank